Structural and magnetic properties of $LiNi_{0.5}Mn_{1.5}O_4$ and $LiNi_{0.5}Mn_{1.5}O_{4-\delta}$ spinels: A first-principles study*

Xin Xiao-Gui(忻晓桂), Shen Jing-Qin(沈静琴), and Shi Si-Qi(施思齐)†

Department of Physics, Center for Optoelectronics Materials and Devices, Zhejiang Sci-Tech University, Xiasha College Park, Hangzhou 310018, *China*

(Received 21 May 2012; revised manuscript received 19 June 2012)

Structural and magnetic properties of $LiNi_{0.5}Mn_{1.5}O_4$ and $LiNi_{0.5}Mn_{1.5}O_{4-\delta}$ are investigated using density-functional theory calculations. Results indicate that nonstoichiometric $LiNi_{0.5}Mn_{1.5}O_{4-\delta}$ and stoichiometric $LiNi_{0.5}Mn_{1.5}O_4$ exhibit two different structures, i.e., the face-centred cubic (*Fd*-3*m*) and primitive, or simple, cubic ($P4_332$) space groups, respectively. It is found that the magnetic ground state of $LiNi_{0.5}Mn_{1.5}O_4$ ($P4_332$ and *Fd*-3*m*) is a ferrimagnetic state in which the Ni and Mn sublattices are ferromagnetically ordered along the [110] direction whereas they are antiferromagnetic with respect to each other. We demonstrate that it is the presence of an O-vacancy in $LiNi_{0.5}Mn_{1.5}O_{4-\delta}$ with the *Fd*-3*m* space group that results in its superior electronic conductivity compared with $LiNi_{0.5}Mn_{1.5}O_4$ with the $P4_332$ space group.

Keywords: $LiNi_{0.5}Mn_{1.5}O_4$, magnetic properties, crystal structures, first-principles calculations

PACS: 82.47.Aa, 31.15.A–, 71.20.–b **DOI:** 10.1088/1674-1056/21/12/128202

1. Introduction

Cathode materials with high energy and power densities have been extensively studied for lithium ion batteries to meet the demands of electric vehicles (EVs) and hybrid electric vehicles (HEVs).[1–4] Among the materials proposed for positive electrodes, lithium manganese oxide spinel has received much attention because of its high energy density, low cost, excellent safety, low toxicity, and so on.[5–8] However, wide application of the $LiMn_2O_4$ cathode is restricted by the capacity fading problem on cycling because of the well-known Jahn–Teller structural distortion of MnO_6 octahedron and the disproportionation reaction of Mn^{3+} ions with the electrolyte during lithium ion intercalation/deintercalation.[9–12] The performance of cathode material $LiMn_2O_4$ can be improved significantly by substituting suitable nontransition or transition metal cations, such as Co, Mg, Cr, Ni, and Cu.[13–17] Among them, $LiNi_{0.5}Mn_{1.5}O_4$ is particularly interesting due to its high operating voltage at $\sim$ 4.7 V versus Li^+/Li, good cycling performances without Jahn–Teller effect related to the presence of Mn^{3+} and good thermal stability.[18–20]

Many experimental investigations on the structural and magnetic properties of $LiNi_{0.5}Mn_{1.5}O_4$ have been carried out. In 1966, magnetic measurement by Blasse[21] indicated that $LiNi_{0.5}Mn_{1.5}O_4$ is a ferrimagnetic spinel material with Ni^{2+} and Mn^{4+} at octahedral sites and Li^+ at tetrahedral sites. Since then, there have been numerous similar investigations[22–26] of ferrimagnetism for $LiNi_{0.5}Mn_{1.5}O_4$ at room temperature. Besides, many research groups have reported that $LiNi_{0.5}Mn_{1.5}O_4$ has two different crystal structures with the *Fd*-3*m* and $P4_332$ space groups.[27–30] Nevertheless, Kim *et al.*[27] argued that stoichiometric $LiNi_{0.5}Mn_{1.5}O_4$ has a primitive, or simple, cubic structure ($P4_332$) while nonstoichiometric $LiNi_{0.5}Mn_{1.5}O_{4-\delta}$ has a normal face-centered spinel structure (*Fd*-3*m*). In addition, Kim *et al.*[27] and Kunduraci and Amatucci[28] have reported that $LiNi_{0.5}Mn_{1.5}O_4$ with the *Fd*-3*m* space group has a superior electrochemical behaviour and structure reversibility compared with $LiNi_{0.5}Mn_{1.5}O_4$ with the $P4_332$ space group. Moreover, Arrhenius plots of sintered pellets by Kunduraci and Amatucci[28] and Kunduraci *et al.*[29] have revealed that the electronic conductivity of $LiNi_{0.5}Mn_{1.5}O_4$ with the $P4_332$ space group is two orders of magnitude lower than that of $LiNi_{0.5}Mn_{1.5}O_4$ with the *Fd*-3*m* space group, and

*Project supported by the National Natural Science Foundation of China (Grant Nos. 51072183 and 50802089) and the Natural Science Foundation of Zhejiang Province, China (Grant No. Y4090280).

†Corresponding author. E-mail: siqishihz@gmail.com

© 2012 Chinese Physical Society and IOP Publishing Ltd

that the difference in electronic conductivity is due to the presence of a small amount of Mn^{3+} in the *Fd*-3*m* space group. However, whether oxygen vacancies affect electronic conductivity is still under debate. In addition, the structures of $LiNi_{0.5}Mn_{1.5}O_4$ and $LiNi_{0.5}Mn_{1.5}O_{4-\delta}$ may affect their electronic conductivity. Therefore, a comprehensive understanding of the structural property and the O-vacancy formation of $LiNi_{0.5}Mn_{1.5}O_4$ ($P4_332$ and *Fd*-3*m*) will be valuable.

On the other hand, there have been some theoretical studies on fundamental properties of $LiNi_{0.5}Mn_{1.5}O_4$. Shi *et al.*[31] investigated the effects of the cation M (M=Cr, Mn, Fe, Co, and Ni) doping on the electronic structure of $LiMn_2O_4$ and found that the origin of the higher intercalation voltage in $LiM_yMn_{2-y}O_4$ can be ascribed to the lower O-2p level introduced by the doping cation M. First-principles calculations by Biškup *et al.*[32] have indicated that in $LiNi_{0.5}Mn_{1.5}O_4$ spinel there is an antiferromagnetic ordering within Mn and Ni, resulting in a ferrimagnetic behaviour. Very recently, first-principles calculations on the stoichiometric spinel $LiNi_{0.5}Mn_{1.5}O_4$ revealed no intermediate phases between $LiNi_{0.5}Mn_{1.5}O_4$ and $Li_0Ni_{0.5}Mn_{1.5}O_4$, indicating that the small step observed in experiment on $LiNi_{0.5}Mn_{1.5}O_4$ with the $P4_332$ space group may be the consequence of partial $LiNi_{0.5}Mn_{1.5}O_{4-\delta}$ with the *Fd*-3*m* space group.[33]

Although some of the interesting results on $LiNi_{0.5}Mn_{1.5}O_4$ have been obtained, to the best of our knowledge, there has been no systematic study on the comparison of electronic structure and magnetic property between stoichiometric $LiNi_{0.5}Mn_{1.5}O_4$ and nonstoichiometric $LiNi_{0.5}Mn_{1.5}O_{4-\delta}$. It is also of great importance to clarify the inherent reason for the more favourable electronic properties of nonstoichiometric $LiNi_{0.5}Mn_{1.5}O_{4-\delta}$ than stoichiometric $LiNi_{0.5}Mn_{1.5}O_4$. In the present paper, we conduct systematic studies of the structural and magnetic properties of $LiNi_{0.5}Mn_{1.5}O_4$ with the $P4_332$ and *Fd*-3*m* space groups using the first-principles all-electron projector augmented wave method based on the state-of-the-art density functional theory.

2. Computational details

Spin-polarized calculations were conducted with the Vienna *ab initio* simulation package (VASP) in the framework of the projector augmented wave method.[34−36] The generalized gradient approximation (GGA) was employed for the exchange–correlation (XC) potential.[37] To account for strong on-site Coulomb repulsion among the Mn-3d and Ni-3d electrons, the Hubbard parameter U was added to the GGA functional in the rotationally invariant approach of Dudarev *et al.*,[38] in which only the difference ($U_{\rm eff} = U - J$) between the Coulomb repulsion U and screened exchange J parameters must be specified. In the present work we chose $U_{\rm eff} = 4.5$ eV for Mn and Ni, as this has been reported to be an appropriate value in Refs. [39] and [40].

Li-$2s^12p^0$, O-$2s^22p^4$, Mn-$3d^64s^1$, and Ni-$3d^94s^1$ were treated as the valence electrons, while all the other electrons were treated as core electrons. In order to avoid the interaction between the two images of the defect due to the periodic boundary condition, we modeled the defect properties using a 56-atom supercell derived from the spinel structure. We used a plane-wave cutoff energy of 500 eV and 2×2×2 Monkhorst–Pack k-point mesh with a Gaussian smearing of 0.20 eV[41] for the defect properties. Atomic positions were fully relaxed and the final force on each atom was less than 0.02 eV·Å^{-1} (1 Å=0.1 nm). These parameters assure a total energy convergence of 2 meV·atom^{-1}. For a more accurate calculation of the electronic density of states (DOS), we used 4×4×4 k-point mesh and the linear tetrahedron method with Blöchl correction.[42]

3. Results and discussion

3.1. Structures of $LiNi_{0.5}Mn_{1.5}O_4$

It is well known that $LiNi_{0.5}Mn_{1.5}O_4$ exhibits two types of crystallographic symmetries,[27−30] i.e., face-centered (*Fd*-3*m*) and primitive, or simple, cubic ($P4_332$) space group. For $LiNi_{0.5}Mn_{1.5}O_4$ with the $P4_332$ space group, Li ions are located at 8*c* sites, Mn ions at 12*d* sites, Ni ions at 4*a* sites, and O ions at 8*c* and 24*e* sites as shown in Fig. 1. Note that herein Ni and Mn ions are regularly ordered. For $LiNi_{0.5}Mn_{1.5}O_4$ with the *Fd*-3*m* space group, however, Li ions are located at 8*a* sites, Mn and Ni ions are randomly distributed in 16*d* sites, and O ions occupy the 32*e* sites as shown in Fig. 2. Note that we use the unit cell of $LiNi_{0.5}Mn_{1.5}O_4$ ($P4_332$ and *Fd*-3*m*) with 32 O ions and 24 cations as shown in Figs. 1 and 2. The experimental lattice parameters[27] for the $P4_332$ and *Fd*-3*m* space groups are 8.166 Å and 8.172 Å, re-

spectively. Therefore, their fundamental difference is where Ni ions are located. However, it is worth mentioning that Ni and Mn ions are identically distributed at 16d sites in $LiNi_{0.5}Mn_{1.5}O_4$ with the *Fd*-3*m* space group.

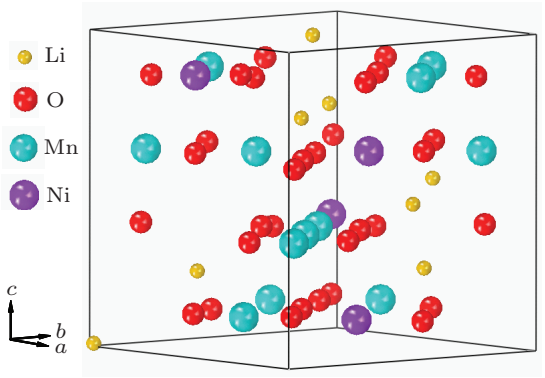


Fig. 1. (colour online) Schematic plot of the crystal structure of $LiNi_{0.5}Mn_{1.5}O_4$ with the $P4_332$ space group. Red, yellow, purple, and blue spheres represent O, Li, Ni, and Mn atoms, respectively.

In order to further gain an insight into the detailed atomic structure of $LiNi_{0.5}Mn_{1.5}O_4$ with the *Fd*-3*m* space group, we consider all the possible configurations. In the supercell (see Fig. 2), there are four Ni ions and twelve Mn ions located at 16d sites. It can be clearly seen that there are sixteen large spheres, which are located in layers 1, 2, 3, and 4 labeled in Fig. 2.

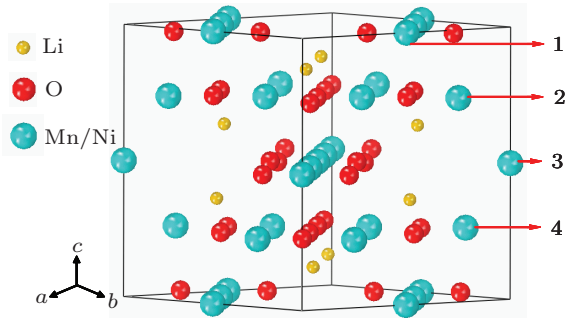


Fig. 2. (colour online) Schematic plot of the crystal structure of $LiNi_{0.5}Mn_{1.5}O_4$ with the *Fd*-3*m* space group. Ni and Mn are located in layers 1, 2, 3, and 4. Red, yellow, and blue spheres represent O, Li, and Ni (Mn) atoms, respectively.

Systematical analyses from structural symmetry and total energy indicate that there are nine types of configurations in total, denoted as Nos. 1∼9 in Table 1.

Table 1 summarizes the lattice parameters, total energies, and relevant average bond lengths for all Ni/Mn distribution-based configurations with the *Fd*-3*m* and $P4_332$ space groups. It is found that for the *Fd*-3*m* space group, No. 4 configuration is energetically the most favourable. Nevertheless, the Ni/Mn distribution mode, lattice parameter, Ni–O bond length, Mn–O bond length, and total energy are the same as those for the $P4_332$ space group (see No. 10 configuration in Table 1). In any case, we can say that No. 4 configuration actually has a primitive, or simple, cubic structure ($P4_332$).

Table 1. All the possible structures, lattice parameters (a_0), total energies (E_{tot}), and relevant bond lengths for $LiNi_{0.5}Mn_{1.5}O_4$ with the $P4_332$ and *Fd*-3*m* space groups.

	No.	a_0/Å	Ni–O/Å	Mn–O/Å	E_{tot}/eV
Fd-3*m*	1	8.304	2.065	1.954	1.903
	2	8.295	2.044	1.953	1.379
	3	8.294	2.069	1.947	0.722
	4	8.290	2.073	1.938	0
	5	8.291	2.062	1.941	0.306
	6	8.296	2.055	1.946	0.925
	7	8.290	2.038	1.954	1.030
	8	8.298	2.062	1.944	1.078
	9	8.294	2.049	1.946	1.438
$P4_332$	10	8.290	2.073	1.938	0

On the other hand, we notice from Table 1 that for the *Fd*-3*m* space group, No. 5 configuration has a total energy 0.306-eV higher than that of No. 4 configuration. This suggests that No. 5 can be chosen as the configuration of $LiNi_{0.5}Mn_{1.5}O_4$ with the *Fd*-3*m* space group, in which Ni ions take up the sites (0.75, 0.25, 0.0), (0.75, 0.75, 0.50), (0.25, 0.50, 0.25), and (0.25, 0.0, 0.75). In other words, stoichiometric $LiNi_{0.5}Mn_{1.5}O_4$ indeed possesses a primitive, or simple, cubic structure ($P4_332$), which is consistent with the available experimental results in Refs. [27]–[29], [33], [43]–[45].

3.2. O-vacancy formation energies in $LiNi_{0.5}Mn_{1.5}O_4$

To identify the structures of $LiNi_{0.5}Mn_{1.5}O_4$ and $LiNi_{0.5}Mn_{1.5}O_{4-\delta}$ ($\delta = 0.125$), we calculate the O vacancy formation energy E_{vac} by

$$E_{vac} = E(\text{cell}_{vac}) + \frac{1}{2}E(O_2) - E(\text{cell}), \qquad (1)$$

where $E(\text{cell}_{vac})$ and $E(\text{cell})$ are the total energies of the optimized supercells with and without an O vacancy, and $E(O_2)$ is the total energy for the ground state of an optimized oxygen molecule in the gas phase. Note that, in the process of the O vacancy

formation, the released O atom is assumed to form an oxygen molecule.

For $LiNi_{0.5}Mn_{1.5}O_4$ with different $P4_332$ and Fd-$3m$ space groups, we consider oxygen–vacancy defects depending on the oxygen atom environmental condition. For oxygen–vacancy defects of $LiNi_{0.5}Mn_{1.5}O_4$ with the $P4_332$ and Fd-$3m$ space groups, we considered two kinds of models, respectively. For the first model with the $P4_332$ and Fd-$3m$ space groups, the O-vacancy is surrounded by one Ni^{2+} and two Mn^{4+} ions (corresponding O-vacancy configurations are denoted as $P4_332$-1 and Fd-$3m$-1 in Table 2, respectively); for the second model with the $P4_332$ and Fd-$3m$ space groups, the O-vacancy is surrounded by three Mn^{4+} ions (corresponding O-vacancy configurations are denoted as $P4_332$-2 and Fd-$3m$-2 in Table 2, respectively.).

Table 2. Calculated O-vacancy formation energies and relevant bond lengths for $LiNi_{0.5}Mn_{1.5}O_4$ with the $P4_332$ and Fd-$3m$ space groups.

Defect style	E_{vac}/eV	Mn–O/Å	Ni–O/Å
$P4_332$-perfect		1.938	2.073
$P4_332$-1	2.189	1.964	2.016
$P4_332$-2	2.722	1.939	2.077
Fd-$3m$-perfect		1.941	2.062
Fd-$3m$-1	1.969	1.969	2.002
Fd-$3m$-2	2.566	1.947	2.052

In order to analyse the O-vacancy defects, we describe the O-vacancy formation energies and relevant bond lengths for $LiNi_{0.5}Mn_{1.5}O_4$ ($P4_332$ and Fd-$3m$) in Table 2. It can be seen that the O-vacancy formation energy is lower for the first model than the second model as 2.189 eV versus 2.722 eV for the $P4_332$ space group and 1.969 eV versus 2.566 eV for the Fd-$3m$ space group. Therefore, the first models of $LiNi_{0.5}Mn_{1.5}O_4$ ($P4_332$ and Fd-$3m$) present energetically favourable structures. In addition, the O-vacancy formation energy of the first model with the Fd-$3m$ space group (1.969 eV) is lower than that (2.189 eV) of the first model with the $P4_332$ space group. This suggests that an oxygen deficiency appearing in $LiNi_{0.5}Mn_{1.5}O_4$ with the Fd-$3m$ space group is more favourable than in $LiNi_{0.5}Mn_{1.5}O_4$ with the $P4_332$ space group. Namely, our calculations reveal that nonstoichiometric $LiNi_{0.5}Mn_{1.5}O_{4-\delta}$ (δ = 0.125) should possess the Fd-$3m$ space group, which is consistent with the experimental results in Refs. [27]–[29], [33], and [45].

In order to analyse the influence of the O-vacancy on electrochemical property, we examine the atomic structure of the O-vacancy in $LiNi_{0.5}Mn_{1.5}O_4$ ($P4_332$ and Fd-$3m$). It is found from Table 2 that the average Mn–O bonds in $LiNi_{0.5}Mn_{1.5}O_4$ ($P4_332$ and Fd-$3m$) with the O-vacancy are longer than those in perfect $LiNi_{0.5}Mn_{1.5}O_4$. The average Mn–O bond is longer for the first model than for the second model as 1.964 Å versus 1.939 Å for the $P4_332$ space group and 1.969 Å versus 1.947 Å for the Fd-$3m$ space group. Moreover, the diffusion pathway of the Li ion in $LiMn_2O_4$ is believed to be a three-dimensional network.[45,46] The Li ion moves from one tetrahedral ($8a$) site to the next by migration through a vacant octahedral ($16c$) site.[33,46] Each $16c$ site is surrounded by six Mn ions, forming an Mn ring in the plane that is perpendicular to the Li ion diffusion pathway. While all vacant octahedral sites and the Li ion migration paths in a spinel such as $LiMn_2O_4$ are equivalent, $LiNi_{0.5}Mn_{1.5}O_4$ ($P4_332$ and Fd-$3m$) create an Ni site and an Mn site, which make the vacant octahedral sites divided. Each $16c$ site is surrounded by Mn and Ni ions, forming a ring in the plane that is perpendicular to the Li ion diffusion pathway in $LiNi_{0.5}Mn_{1.5}O_4$ ($P4_332$ and Fd-$3m$). It is obvious that the average Ni–O bond lengths are larger than the average Mn–O ones in Table 2, suggesting that one of the factors influencing the Li ion diffusion should be the Mn–O bond. Actually, the average Mn–O bond lengths for the first model of $LiNi_{0.5}Mn_{1.5}O_{4-\delta}$ ($\delta = 0.125$) ($P4_332$ and Fd-$3m$) are larger than those for stoichiometric $LiNi_{0.5}Mn_{1.5}O_4$, indicating that the former may have a wider Li ion channel.

In order to show how the electrons are distributed in $LiNi_{0.5}Mn_{1.5}O_{4-\delta}$ (δ = 0.125) with the Fd-$3m$ space group, we plot the partial densities of states of Mn-3d for $LiNi_{0.5}Mn_{1.5}O_4$ without and with an O vacancy as shown in Fig. 3. It is found that e_g orbits in the majority spin channel of two Mn atoms are further split in $LiNi_{0.5}Mn_{1.5}O_4$ with the O-vacancy, which brings down the Mn d_{z^2} orbits and opens a gap of about 0.4 eV between the Mn d_{z^2} and the Mn $d_{x^2-y^2}$ as in Fig. 3(a). The lowered d_{z^2} orbits become filled and the corresponding Mn atoms become Mn^{3+}, which is Jahn–Teller active.[40] In other words, the

formation of the O vacancy in $LiNi_{0.5}Mn_{1.5}O_4$ causes the two excess electrons to preferentially occupy Mn-3d states, resulting in the reduction of Mn^{4+} to Mn^{3+}, although the oxidation state of Mn in $LiNi_{0.5}Mn_{1.5}O_4$ ($P4_332$ and Fd-$3m$) is fixed at +4. This is consistent with the suggestion in Refs. [16] and [47], i.e., an oxygen deficiency appearing in $LiNi_{0.5}Mn_{1.5}O_4$ should lower the Mn oxidation state from Mn^{4+} to Mn^{3+}.

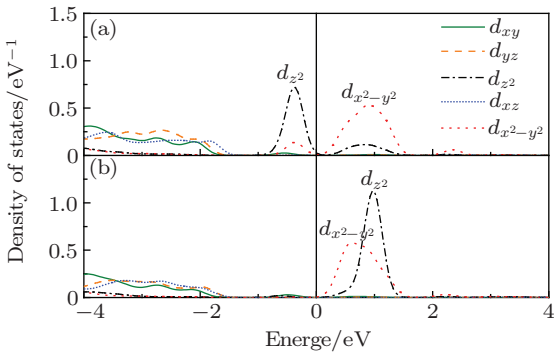


Fig. 3. (colour online) Majority-spin Mn-3d projected density of states of (a) Mn^{3+} in $LiNi_{0.5}Mn_{1.5}O_{4-\delta}$ ($\delta = 0.125$) with the Fd-$3m$ space group and (b) Mn^{4+} in $LiNi_{0.5}Mn_{1.5}O_4$ with the Fd-$3m$ space group. The Fermi level is set to be zero eV.

Figure 4 shows the partial densities of states (PDOSs) for the ferrimagnetic $LiNi_{0.5}Mn_{1.5}O_4$ ($P4_332$ and Fd-$3m$) and $LiNi_{0.5}Mn_{1.5}O_{4-\delta}$ ($\delta = 0.125$) (Fd-$3m$). It can be seen that the electronic states around the Fermi level are mainly (almost all) contributed to by Mn-3d, Ni-3d, and O-2p. Once $LiNi_{0.5}Mn_{1.5}O_4$ with the Fd-$3m$ space group is reduced by removing an O atom, a new peak emerges in the Mn-3d orbit around the Fermi level. The special electronic structure around the Fermi level may cause higher electronic conductivity of $LiNi_{0.5}Mn_{1.5}O_{4-\delta}$ ($\delta = 0.125$). Also, the comparison between the electronic structures of stoichiometric $LiNi_{0.5}Mn_{1.5}O_4$ with the $P4_332$ and Fd-$3m$ space groups reveals that the PDOSs for $LiNi_{0.5}Mn_{1.5}O_4$ with the $P4_332$ and Fd-$3m$ space groups are almost identical. Therefore, $LiNi_{0.5}Mn_{1.5}O_{4-\delta}$ with the Fd-$3m$ space group has superior electronic conductivity compared with $LiNi_{0.5}Mn_{1.5}O_4$ with the $P4_332$ space group because of the presence of oxygen deficiency in the former, which is in good agreement with the experimental conclusions.[27–29] As is well known, $LiMn_2O_4$ suffers from a fast capacity fade because of the existence of Jahn–Teller active ions, Mn^{3+}.[9–11] However, it is interesting that although Mn^{3+} ions are present in $LiNi_{0.5}Mn_{1.5}O_{4-\delta}$ ($\delta = 0.125$) with the Fd-$3m$ space group, this material exhibits better electrochemical performance than $LiNi_{0.5}Mn_{1.5}O_4$ with the $P4_332$ space group, which is considered to have only Mn^{4+} in its oxide matrix.

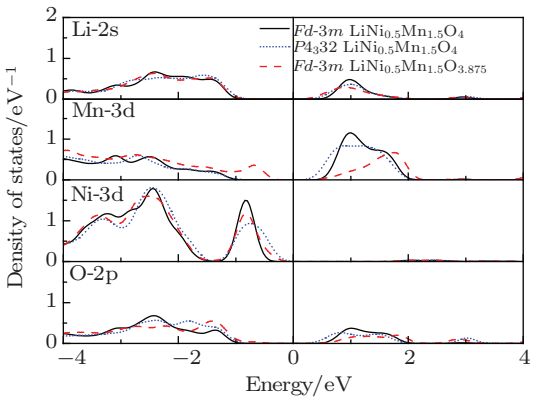


Fig. 4. (colour online) Partial densities of states of the ferrimagnetic $LiNi_{0.5}Mn_{1.5}O_4$ ($P4_332$ and Fd-$3m$) and $LiNi_{0.5}Mn_{1.5}O_{4-\delta}$ ($\delta = 0.125$) (Fd-$3m$). The zero point of the energy axis corresponds to the Fermi level.

3.3. Magnetic properties of $LiNi_{0.5}Mn_{1.5}O_4$

In order to exactly study the magnetic properties of $LiNi_{0.5}Mn_{1.5}O_4$ with the $P4_332$ and Fd-$3m$ space groups, the calculations are performed for the four different spin configurations, i.e., ferrimagnetic, ferromagnetic, antiferromagnetic, and nonmagnetic states, (denoted as GGA-FiM, GGA-FM, GGA-AFM, and GGA-NM, respectively, see Table 3). Figures 5(a) and 5(b) show the antiferromagnetic spin configurations of $LiNi_{0.5}Mn_{1.5}O_4$ with the Fd-$3m$, and $P4_332$ space groups. In the ferrimagnetic configurations of $LiNi_{0.5}Mn_{1.5}O_4$ (Fd-$3m$ and $P4_332$), the Mn and Ni ions along the [110] direction are both antiparallelly arranged sequentially as shown in Figs. 6(a) and 6(b). It is obvious to see from Table 3 that the ferrimagnetic configuration of $LiNi_{0.5}Mn_{1.5}O_4$ with the $P4_332$ space group has total energies of 0.361 eV, 0.552 eV, and 37.000 eV, lower (per supercell) than those of the ferromagnetic, antiferromagnetic, and nonmagnetic configurations, respectively. The ferrimagnetic configuration of $LiNi_{0.5}Mn_{1.5}O_4$ with the Fd-$3m$ space group also has total energies of 0.055 eV, 0.095 eV, and 37.080 eV, lower (per supercell) than those of the ferromagnetic, antiferromagnetic, and nonmagnetic configurations, respectively. Consequently, the magnetic ground state of $LiNi_{0.5}Mn_{1.5}O_4$ (Fd-$3m$ and $P4_332$) is ferrimagnetic, which is consistent with the experimental results in Refs. [21]–[26].

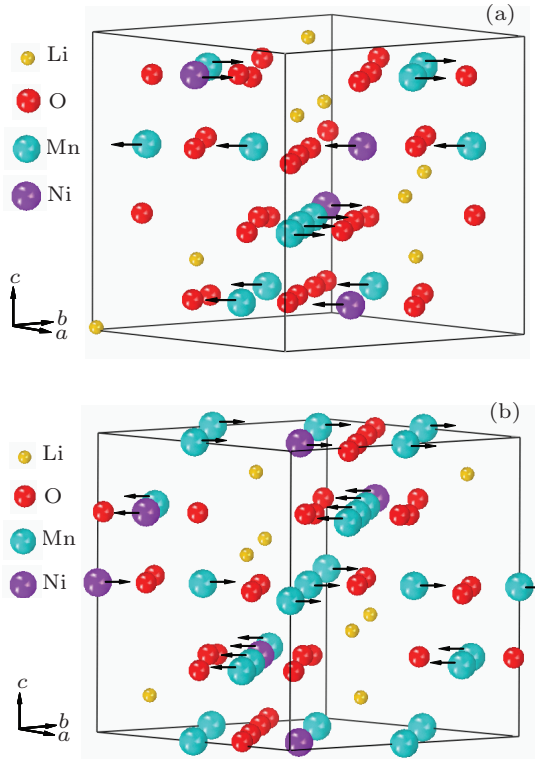


Fig. 5. (colour online) Antiferromagnetic spin configurations of $LiNi_{0.5}Mn_{1.5}O_4$ with (a) $P4_332$ and (b) Fd-$3m$ space groups. Red, yellow, purple, and blue spheres represent O, Li, Ni, and Mn atoms, respectively.

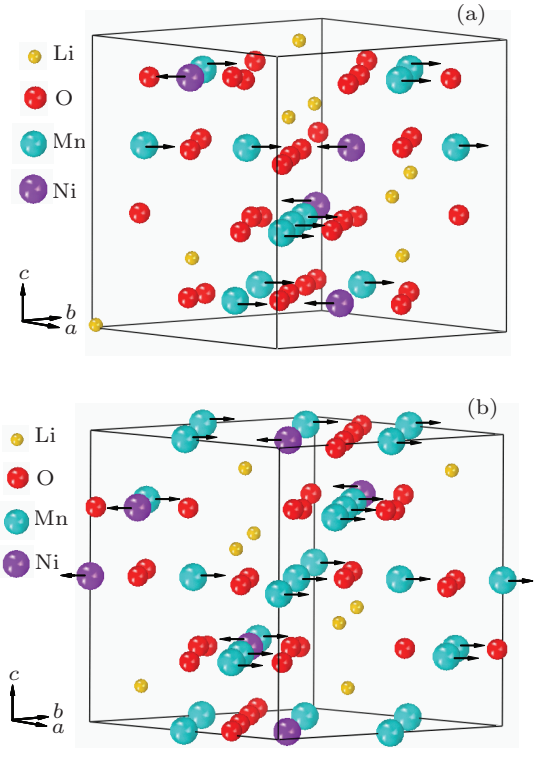


Fig. 6. (colour online) Ferrimagnetic spin configurations of $LiNi_{0.5}Mn_{1.5}O_4$ with (a) $P4_332$ and (b) Fd-$3m$ space groups. Red, yellow, purple, and blue spheres represent O, Li, Ni, and Mn atoms, respectively.

Table 3. Lattice parameters (a_0) and total energies (E_{tot}) for ferrimagnetic, ferromagnetic, antiferromagnetic, and nonmagnetic configurations (denoted as GGA-FiM, GGA-FM, GGA-AFM, and GGA-NM, respectively) in $LiNi_{0.5}Mn_{1.5}O_4$ with the $P4_332$ and Fd-$3m$ space groups.

		Exp.[27]	GGA-FiM	GGA-FM	GGA-AFM	GGA-NM
Fd-$3m$	a_0/Å	8.172	8.291	8.293	8.290	8.177
	E_{tot}/eV		0	0.055	0.095	37.080
$P4_332$	a_0/Å	8.166	8.290	8.293	8.285	7.987
	E_{tot}/eV		0	0.361	0.552	37.000

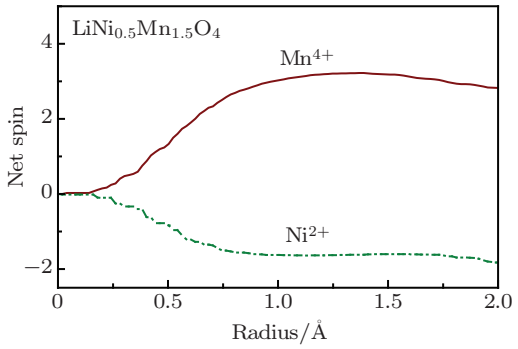


Fig. 7. (colour online) Curves of integrated spin versus integration radius (Å) around Ni and Mn ions in $LiNi_{0.5}Mn_{1.5}O_4$ (Fd-$3m$) with ferrimagnetic spin configuration.

To further understand the magnetic ground-state properties, we plot the curves of integrated spin versus sphere radius around Ni and Mn ions in $LiNi_{0.5}Mn_{1.5}O_4$ (Fd-$3m$ and $P4_332$). It can be clearly seen from Fig. 7 that the plateau in $LiNi_{0.5}Mn_{1.5}O_4$ with the Fd-$3m$ space group gives a net spin density of about 3.2 μ_B for Mn and about 1.6 μ_B for Ni, which correspond to the values of net spins of Mn^{4+} and Ni^{2+}. In addition, the spin moments of Mn^{4+} and Ni^{2+} ions in $LiNi_{0.5}Mn_{1.5}O_4$ with the Fd-$3m$ space group have opposite signs, indicating an antiferromagnetic coupling between Mn^{4+} and Ni^{2+} ions. In other words, both Mn^{4+}–O^{2-}–Mn^{4+} and Ni^{2+}–O^{2-}–Ni^{2+} couplings are ferromagnetic whereas Mn^{4+}–O^{2-}–Ni^{2+} is an antiferromagnetic coupling along the [110] direction, which has been experimentally observed.[21–26] Consequently, the above discussion clearly shows that

it is the antiferromagnetic coupling between the Mn^{4+} and Ni^{2+} ions that leads to the ferrimagnetism in $LiNi_{0.5}Mn_{1.5}O_4$ (Fd-3m and $P4_332$). The ferrimagnetic model of $LiNi_{0.5}Mn_{1.5}O_4$ (Fd-3m and $P4_332$) has a magnetic moment of 28 μ_B, which is consistent with the experimental value reported by Blasse.[21]

4. Conclusions

Using the first-principles density-functional theory and considering the on-site Coulomb interaction within the GGA+U scheme, we investigate crystal structures and magnetic properties of $LiNi_{0.5}Mn_{1.5}O_4$ and $LiNi_{0.5}Mn_{1.5}O_{4-\delta}$. The results indicate that stoichiometric and nonstoichiometric $LiNi_{0.5}Mn_{1.5}O_4$ have two different structures ($P4_332$ and Fd-3m). Ferromagnetic orderings of Ni and Mn sublattices in $LiNi_{0.5}Mn_{1.5}O_4$ ($P4_332$ and Fd-3m) along the [110] direction and their antiferromagnetic ordering relative to each other result in its ferrimagnetic magnetic ground state. It is confirmed that the $LiNi_{0.5}Mn_{1.5}O_{4-\delta}$ with the Fd-3m space group has superior electronic conductivity compared with the $LiNi_{0.5}Mn_{1.5}O_4$ with the $P4_332$ space group because of the oxygen deficiency in the former.

References

[1] Wu X L, Jiang L Y, Cao F F, Guo Y G and Wan L J 2009 *Adv. Mater.* **21** 2710
[2] Shi S L, Liu Y G, Zhang J Y and Wang T H 2009 *Chin. Phys.* B **18** 4564
[3] Hou X H, Hu S J, Li W S, Ru Q, Yu H W and Huang Z W 2008 *Chin. Phys.* B **17** 3422
[4] Chen Y C, Xie K, Pan Y, Zheng C M and Wang H L 2011 *Chin. Phys.* B **20** 028201
[5] Tarascon J M and Guyomard D 1993 *Electrochim. Acta* **38** 1221
[6] Guyomard D and Tarascon J M 1994 *Solid State Ionics* **69** 222
[7] Sun X, Yang X Q, Balasubramanian M, McBreen J, Xia Y and Sakai T 2002 *J. Electrochem. Soc.* **149** A842
[8] Saitoh M, Sano M, Fujita M, Sakata M, Takata M and Nishibori E 2004 *J. Electrochem. Soc.* **151** A17
[9] Tarascon J M, Mckinnon W R, Coowar F, Boowner T N, Amatucci G and Guyomard D 1997 *J. Electrochem. Soc.* **22** 141
[10] Yamaguchi H, Yamada A and Uwe H 1998 *Phys. Rev.* B **58** 8
[11] Choi W and Manthiram A 2006 *J. Electrochem. Soc.* **153** A1760
[12] Thackeray M M 1997 *Prog. Solid State Chem.* **25** 1
[13] Arora P, Popov B and White R E 1998 *J. Electrochem. Soc.* **145** 807
[14] Takahashi M, Yoshida T, Ichikawa A, Kitoh K, Katsukawa H, Zhang Q and Yoshio M 2006 *Electrochim. Acta* **51** 5508
[15] Li G H, Ikuta H, Uchida T and Wakihara M 1996 *J. Electrochem. Soc.* **143** 178
[16] Zhong Q, Bonakdarpour A, Zhang M, Gao Y and Dahn J R 1997 *J. Electrochem. Soc.* **144** 205
[17] Ein-Eli Y, Howard W F, Lu S H, Mukerjee S, Mcbreen J, Vaughey J T and Thackeray M M 1998 *J. Electrochem. Soc.* **145** 1238
[18] Kim J H, Myung S T and Sun Y K 2004 *Electrochim. Acta* **49** 219
[19] Patoux S, Sannier L, Lignier H, Reynier Y, Bourbon C, Jouanneau S, Cras F L and Martinet S 2008 *Electrochim. Acta* **53** 4137
[20] Wang L P, Li H, Huang X J and Baudrin E 2011 *Solid State Ionics* **193** 32
[21] Blasse G 1966 *J. Phys. Chem. Solids* **27** 383
[22] Goodenough J B 1963 *Magnetism and the Chemical Bond* (New York: Wiley)
[23] Branford W, Green M A and Neumann D A 2002 *Chem. Mater.* **14** 1649
[24] Lee Y J, Eng C and Grey C P 2001 *J. Electrochem. Soc.* **148** A249
[25] Nakamura T, Yamada Y and Tabuchi M 2005 *J. Appl. Phys.* **98** 093905
[26] Amdouni N, Zaghib K, Gendron F, Mauger A and Julien C M 2007 *J. Magn. Magn. Mater.* **309** 100
[27] Kim J H, Myung S T, Yoon C S, Kang S G and Sun Y K 2004 *Chem. Mater.* **16** 906
[28] Kunduraci M and Amatucci G G 2006 *J. Electrochem. Soc.* **153** A1345
[29] Kunduraci M, Al-Sharab J F and Amatucci G G 2006 *Chem. Mater.* **18** 3585
[30] Ariyoshi K, Iwakoshi Y, Nakayama N and Ohzuku T 2004 *J. Electrochem. Soc.* **151** A296
[31] Shi S Q, Ouyang C Y, Wang D S, Chen L Q and Huang X J 2003 *Solid State Commun.* **126** 531
[32] Biškup N, Martínez J L, Arroyo Y, de Dompablo M E, Díaz-Carrasco P and Morales J 2006 *J. Appl. Phys.* **100** 093908
[33] Xia H, Meng Y S, Lu L and Ceder G 2007 *J. Electrochem. Soc.* **154** A737
[34] Blöchl P E 1994 *Phys. Rev.* B **50** 17953
[35] Kresse G and Joubert D 1999 *Phys. Rev.* B **59** 1758
[36] Kresse G and Furthmüller J 1996 *Comput. Mater. Sci.* **6** 15
[37] Perdew J P, Chevary J A, Vosko S H, Jackson K A, Pederson M R, Singh D J and Fiolhais C 1992 *Phys. Rev.* B **46** 6671
[38] Dudarev S L, Botton G A, Savrasov S Y, Humphreys C J and Sutton A P 1998 *Phys. Rev.* B **57** 1505
[39] Zhou F, Kang K, Maxisch T, Ceder G and Morgan D 2004 *Solid State Commun.* **132** 181
[40] Ouyang C Y, Du Y L, Shi S Q and Lei M S 2009 *Phys. Lett.* A **373** 2796
[41] Methfessel M and Paxton A T 1989 *Phys. Rev.* B **40** 3616
[42] Blöchl P E, Jepsen O and Andersen O K 1994 *Phys. Rev.* B **49** 16223
[43] Takahashi K, Saitoh M, Sano M, Fujita M and Kifune K 2004 *J. Electrochem. Soc.* **151** A173
[44] Alcántara R, Jaraba M, Lavela P, Tirado J L, Zhecheva E and Stoyanova R 2004 *Chem. Mater.* **16** 1573
[45] Wakihara M 2005 *Electrochemistry* (Tokyo, Jpn.) **73** 328
[46] Ammundsen B, Rozière J and Islam M S 1997 *J. Phys. Chem.* B **101** 8156
[47] Ma X H, Kang B and Ceder G 2010 *J. Electrochem. Soc.* **157** A925